



This is a repository copy of *Use of electrical impedance spectroscopy for intraoperative tissue differentiation during thyroid and parathyroid surgery.*

White Rose Research Online URL for this paper:
<http://eprints.whiterose.ac.uk/153307/>

Version: Published Version

Article:

Hillary, S.L., Brown, B.H., Brown, N.J. orcid.org/0000-0002-2100-1905 et al. (1 more author) (2019) Use of electrical impedance spectroscopy for intraoperative tissue differentiation during thyroid and parathyroid surgery. *World Journal of Surgery*. ISSN 0364-2313

<https://doi.org/10.1007/s00268-019-05169-7>

Reuse

This article is distributed under the terms of the Creative Commons Attribution (CC BY) licence. This licence allows you to distribute, remix, tweak, and build upon the work, even commercially, as long as you credit the authors for the original work. More information and the full terms of the licence here:
<https://creativecommons.org/licenses/>

Takedown

If you consider content in White Rose Research Online to be in breach of UK law, please notify us by emailing eprints@whiterose.ac.uk including the URL of the record and the reason for the withdrawal request.



eprints@whiterose.ac.uk
<https://eprints.whiterose.ac.uk/>



Use of Electrical Impedance Spectroscopy for Intraoperative Tissue Differentiation During Thyroid and Parathyroid Surgery

Sarah L. Hillary¹ · Brian H. Brown¹ · Nicola J. Brown¹ · Saba P. Balasubramanian²

© The Author(s) 2019

Abstract

Background Electrical impedance (EI) measures tissue resistance to alternating current across several frequencies and may help identify tissue type. A recent rabbit model demonstrated that electrical impedance spectroscopy (EIS) may facilitate identification of parathyroid glands and potentially improve outcomes following surgery. This study looks at the EI patterns of soft tissues in the human neck to determine whether parathyroid tissue can be accurately identified.

Methods This was a phase 1, single-arm interventional study involving 56 patients undergoing thyroid and/or parathyroid surgery. Up to 12 EI readings were taken from in vivo and ex vivo thyroid and parathyroid glands, adipose tissue and muscle of each patient. Each reading consists of a series of measurements over 14 frequencies from each tissue. EI patterns were analysed. Two patients were excluded due to data loss due to device malfunction.

Results The median age of participants was 53.5 (range 20–85) years. Thirty-five participants had surgery for thyroid pathology, 17 for parathyroid pathology and four for both. Six hundred and six EIS spectra were reviewed for suitability. One hundred and eighty-four spectra were rejected leaving 422 spectra for analysis. The impedance patterns of the soft tissues differed by histological type. The EI ratio of low (152 Hz) to high (312 kHz) frequencies demonstrated a significant difference between the soft tissues ($p = 0.006$). Using appropriate thresholds, parathyroid tissue can be distinguished from thyroid tissue with a sensitivity of 76% and specificity of 60%.

Conclusions This study demonstrates the feasibility of using EIS to aid parathyroid identification and preservation. Further changes to the device and modelling of the EI patterns across the range of frequencies may improve accuracy and facilitate intraoperative use.

Trial registration ClinicalTrials.gov (NCT02901873).

Introduction

Electrical impedance spectroscopy (EIS) measures the resistance to an electrical circuit over a range of frequencies. When tissue is placed as part of the circuit, the resistance or impedance spectrum across a range of frequencies can be specific to that tissue type. EIS can detect changes in the shape and structure of the cells within the tissue [1–3]. This property has been used to aid the early detection of cervical cancer [1, 2, 4] and is being explored in the oral cavity to detect oral cancer and its potential use

This paper was presented as an oral presentation at the IAES meeting/48th World Congress of Surgery August 11–15, 2019 in Kraków, Poland.

✉ Sarah L. Hillary
sarah.hillary@doctors.org.uk

¹ University of Sheffield, Sheffield, UK

² Sheffield Teaching Hospitals NHS Foundation Trust,
University of Sheffield, Sheffield, UK



Fig. 1 ZedScan™ portable handset and docking station. The user screen is visible on the hand piece, and LED lights are halfway down the nose cone. A single-use cover is placed over the nose cone for use in humans

in detection of multiple sclerosis [5–7]. Other early studies have investigated its ability to identify cancer in prostate, bladder and breast tissues [8–14].

Impedance differences between tissues such as the thyroid and parathyroid could be exploited to help surgeons in the intraoperative identification of parathyroid glands. Early confirmation that tissue is indeed a parathyroid gland would aid preservation of the tissue and has potential to reduce the incidence and/or severity of post-surgical hypoparathyroidism [15] after thyroid and/or parathyroid surgery. It would particularly be of use in patients undergoing redo surgery or central compartment lymphadenectomy, where the risk of post-surgical hypoparathyroidism (PoSH) is higher than usual [15]. PoSH is associated with significant short- and long-term morbidity [16] and mortality [16].

In a rabbit model evaluating the EI spectra of soft tissue structures in the neck, a clear difference in EI spectra between thyroid and parathyroid tissues was demonstrated [17]. The study also found that the ratio of low (152 Hz) to high (312 kHz) frequency of in situ thyroid, parathyroid and muscle was found to be significantly different. The electrical impedance (EI) of ex vivo tissue was significantly higher than the corresponding in vivo readings, probably due to temperature differences, as impedance rises by approximately 2% per degree centigrade fall in temperature [18].

The aim of this study was to determine the EI spectra of normal and abnormal human thyroid, parathyroid, adipose tissue and muscle; to compare the EI patterns of the parathyroid with the other soft tissue structures; and to investigate changes in EI before and immediately after excision of soft tissue structures in thyroid and parathyroid surgery.

Patients and methods

This study is a prospective, single-arm clinical trial conducted at Sheffield Teaching Hospital NHS Foundation Trust between July 2016 and March 2017. All patients aged

18 years and over who were undergoing thyroid and/or parathyroid surgery were eligible to be included in the study. Exclusion criteria included inability to understand spoken and written English, inability to give adequate informed consent or a positive pre-operative pregnancy test.

Eligible patients had the study explained and were given an information sheet when placed on the waiting list for thyroid and/or parathyroid surgery. They were reviewed on the day of surgery, and a further consultation was carried out to confirm eligibility and obtain informed written consent.

The ZedScan™ (Zilico™, Manchester, UK) is a handheld EIS device. A disposable, single-use sensor cover is placed over the nose cone and tip of the hand-held unit (Fig. 1). The diameter of the circular tip is 5.5 mm and has four gold electrodes positioned in a square arrangement. The diameter and spacing of the four electrodes determine the flow of current across the tissue. The current (<12 μ A p–p) is passed between one adjacent pair of electrodes, and the impedance is measured between the second pair. Each reading (taken in 20 ms) from one point on a tissue is a series of impedance measurements over 14 different frequencies (ranging from 76–625,000 Hz).

The procedures were performed by two consultant endocrine surgeons who had been trained in the use of the device. At operation, the surgeons identified the thyroid and parathyroid glands as per standard practice. The EIS device was placed in a sterile cover, and up to 12 readings were taken from the structures identified in the neck including thyroid, parathyroid gland, muscle, superficial subcutaneous fat and visceral brown fat such as thymus. Abnormal glands were removed at the surgeon's discretion based on their morphological appearance, and ex vivo EIS and temperature readings were taken from excised tissues prior to processing for histological analysis. The EIS data were not available to the surgeons intraoperatively and did not influence the decision on gland excision. The glands from which readings were taken, whether the surgeon

deemed them to be normal or abnormal based on appearance and any specific characteristics of these glands were documented.

The device was docked and the raw data downloaded to a Microsoft Excel spreadsheet. Histology results from the specimens taken were retrieved from the hospital reporting systems. For this study, the raw data were analysed manually as the current software is designed to analyse cervical tissue.

The software installed on the ZedScanTM is meant for use in colposcopy and applies quality control checks allowing data that fall within accepted parameters for cervical tissue to be collected. If the measurements collected do not fulfil the criteria, it repeats the measurements or rejects the reading and prompts the user to reposition and repeat the reading. These checks were initially removed to allow all data to be 'accepted' by the device and collected for analysis. However, it became apparent that the same quality control parameters could also be applied to the data collected from the neck, improving the quality of the data collected, reducing false readings which would later be excluded with resultant loss of data. The internal quality control checks were therefore subsequently reinstated.

The primary outcomes were EIS patterns of the different soft tissue structures in the human neck. The objectives were to determine differences between EIS of parathyroid tissue versus other structures, differences between normal and abnormal parathyroid tissue and differences between vascularised glands (in situ) and devascularised glands (ex vivo).

Data were analysed using SPSS (IBM SPSS Statistics, version 25.0. Armonk, NY: IBM Corp.) and PRISM (GraphPad Software Inc., La Jolla, CA, USA). Data analyses were primarily descriptive. Low to high EI ratios were compared using Friedman's two-way analysis of variance by ranks test. Data were considered to be significantly different if $p \leq 0.05$. Scatter plots and ROC curves were plotted using PRISM.

The study was approved by the regional research ethics committee (REC) (Reference: 15/YH/0293) and the local research and development department (Reference: STH18736). The study protocol was registered with ClinicalTrials.gov [19]. All patients included in the study were fully informed and gave written consent. Privacy and confidentiality were ensured in keeping with Good Clinical Practice guidelines.

Results

Eighty patients were screened for eligibility in outpatient clinic and accepted a participant information sheet. The research team was not available on the day of surgery for

ten patients, and a further ten patients had not been allocated a date for surgery by the end of the study. Sixty patients were approached for a second time on the day of their operation to confirm eligibility and gain written consent. Four patients declined consent.

Fifty-six patients participated in the study (nine males and 47 females). The median (range) age of participants was 53.5 (20–85) years. Thirty-five participants had surgery for thyroid pathology; 17 for parathyroid pathology; and four had surgery for both thyroid and parathyroid pathology. Two patients (one from thyroid and one from parathyroid groups) were subsequently excluded from the study as the device failed intraoperatively with loss of data before docking. In the interest of keeping the anaesthetic time as short as possible in line with the protocol and as the surgeons had continued to operate while the machine was docked, it was decided not to repeat the entire set of readings.

The thyroid operations included hemithyroidectomy for a thyroid nodule ($n = 24$), completion thyroidectomy for cancer ($n = 1$) and total thyroidectomy for Graves' disease ($n = 9$), multinodular goitre ($n = 4$) and cancer ($n = 1$). Table 1 describes the histological diagnosis in these patients. All parathyroid operations were done for primary hyperparathyroidism.

Of 28 'parathyroid glands' sent for histology (excluding one inadvertent parathyroid gland excision during a thyroid lobectomy), 19 were confirmed to be adenomas, six were reported as parathyroid hyperplasia, two were reported to be 'normal' and one was reported to be 'thymus'.

Some spectral readings were rejected if negative values were recorded or if the impedance rose with frequency. The cause of these phenomena is likely to have been poor electrode contact with the tissue. The majority of rejected spectra ($n = 184$) were those taken from fat and muscle. Readings taken before and after the second set of QC checks showed that the number of rejected readings reduced from 39% to 20.0% (Table 2). The 422 readings available for analysis were stratified by patient and tissue type. If there were multiple readings from one tissue type, the average (mean) of the readings was used. This produced 216 spectra for analysis.

Comparisons of EIS spectra were made between parathyroid glands and other tissues in the neck; between normal and abnormal parathyroid glands; and between in vivo (that are likely to be vascularised) and ex vivo (devascularised, recently excised) tissues (Fig. 2). Normal and abnormal thyroid spectra were analysed together as they were similar, and the study was not designed to differentiate between thyroid pathology.

The spectra obtained from human tissue showed lower impedances and greater variability in amplitude than that reported in the rabbit model [17]. Possible causes for this may include the presence of blood around the tissues;

Table 1 Operation and histological diagnosis

Operation	Number	Histological diagnosis	Number
Hemithyroidectomy	24	Thyroid adenoma	10
		Thyroid carcinoma	4
		Thyroid hyperplasia	2
		Multinodular/colloid	8
Total thyroidectomy	14	Graves' disease	9
		Multinodular goitre	3
		Toxic nodular goitre	1
		Thyroid carcinoma	1
Completion thyroidectomy	1	Follicular adenoma	1
Parathyroidectomy	21	Parathyroid adenoma	19
		Parathyroid hyperplasia	2

Table 2 Number of readings taken and rejected before and after internal quality control checks implemented

	Before QC checks applied			After QC checks applied		
	Readings taken	Readings rejected	Rejected (%)	Readings taken	Readings rejected	Rejected (%)
Thyroid	67	11	16	60	2	3
Normal parathyroid	65	22	34	60	14	23
Abnormal parathyroid	15	3	20	27	4	15
Superficial fat	27	20	74	5	2	40
Visceral fat	25	10	40	10	5	50
Muscle	26	21	81	25	13	52
Ex vivo thyroid	64	21	33	64	10	16
Ex vivo parathyroid	22	13	59	31	8	26
Other	12	5	42	1	0	0
Total	323	126	39	283	58	20

difficulty placing the probe flat on the tissue of interest; and the differences in volume of tissues. To remove this variability and to enable direct comparisons of the shape of the spectra, the data were normalised to the mean amplitude of each spectrum over all frequencies. (Fig. 3).

As demonstrated in rabbits [17], in this human study there is a significant difference in ratios of EI at low (152 Hz) to high (312 kHz) frequencies between thyroid, normal parathyroid and muscle (Fig. 4; Friedman's two-way analysis of variance by ranks test; $p = 0.006$).

The impedance of different human tissues at low and high frequencies is similar but the way the impedance changes over the frequencies does appear to be different. The impedance of the thyroid starts to decrease at a lower frequency compared to the parathyroid producing an inverse sigmoid-shaped spectrum. The parathyroid maintains a higher impedance over more of the lower frequencies, and the drop in impedance occurs at a later stage. These patterns in humans are similar to those reported in rabbits and may help differentiate parathyroid tissue from the other tissues in the neck.

The median normalised 'normal parathyroid' spectrum was used to form a template to which the other normalised spectra were compared by template matching. The template match is the deviation from the template expressed as a fraction expressed as a number between 0 and 1. The closer the value is to 0, the closer the spectrum matches the template. This is a similar process to that used in cervical and oral malignancy studies [1, 5]. Receiver operating characteristic (ROC) curves derived from template matching and used to calculate the sensitivity and specificity [3] showed that thyroid and parathyroid tissue can be distinguished with a sensitivity of 76% and specificity of 60% (Fig. 5).

Discussion

This is the first study that examined electrical impedance (EI) properties of soft tissue structures in the human neck in an attempt to distinguish between parathyroid glands and other tissues. As demonstrated, EI of human spectra is

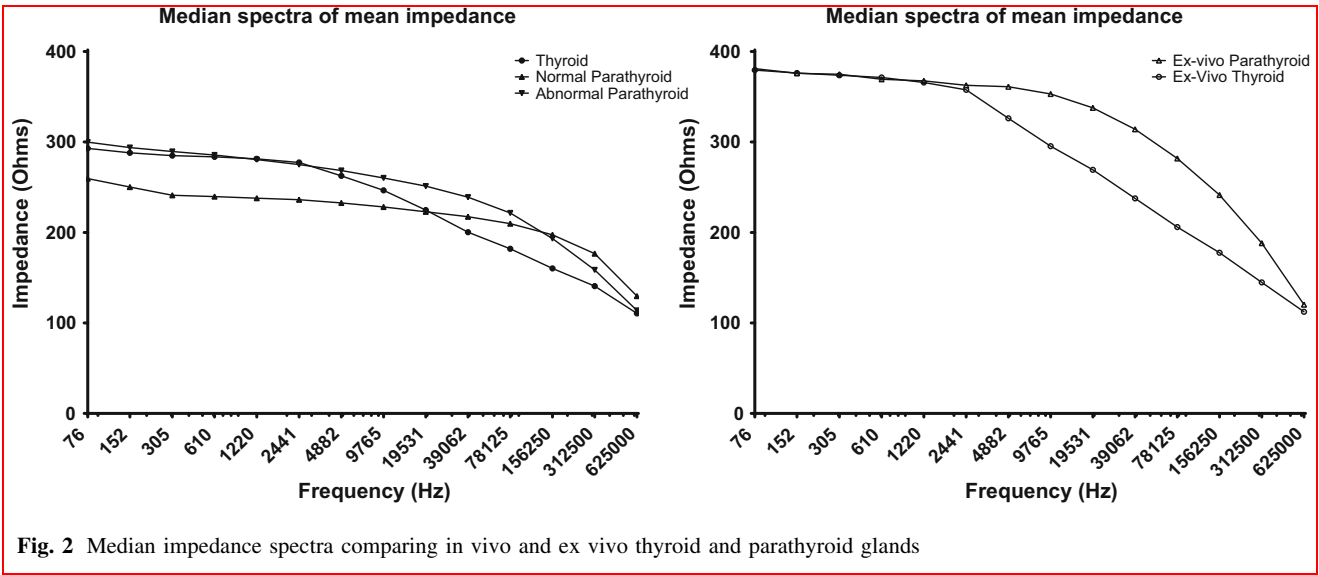


Fig. 2 Median impedance spectra comparing in vivo and ex vivo thyroid and parathyroid glands

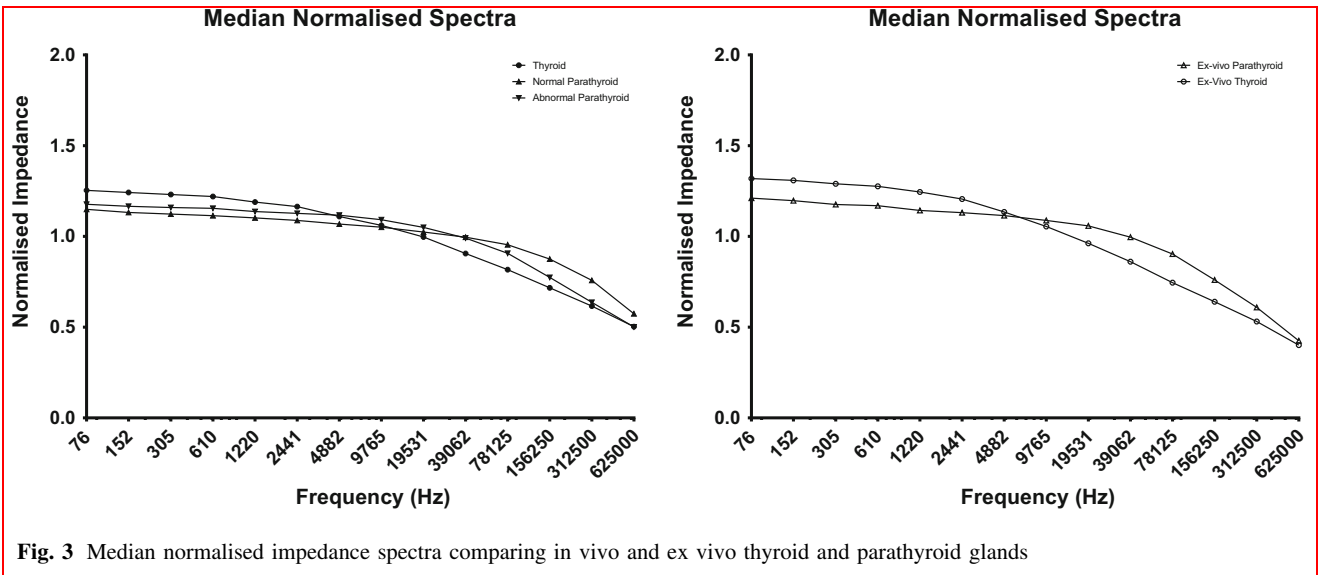


Fig. 3 Median normalised impedance spectra comparing in vivo and ex vivo thyroid and parathyroid glands

similar to that of rabbits previously reported [17], and there were differences in the spectra between parathyroid and thyroid glands.

All abnormal parathyroid glands identified as a parathyroid tissue at surgery and excised were confirmed on histology. One gland that was suspected to be ‘parathyroid’ was shown on histology to be thymic tissue. As normal parathyroid glands were neither excised nor biopsied, the final diagnosis of ‘normal’ tissue is reliant on surgical judgement.

The template used in matching was based on internal study data, allowing increased matching of the parathyroid spectra to the median of all the parathyroid spectra but if there was no concordance in the shape of the spectra

obtained from parathyroid glands, the degree of template matching would still be low.

In clinical practice, one of the difficulties surgeons find is distinguishing parathyroid glands from fat or lymph nodes. Although it was part of the initial aim of this study to compare parathyroid data to these other tissue types, the amount of data collected from these tissues in this study was too small for meaningful comparisons to be made. This would need to be investigated further in a larger study.

The difference in EI spectra between the thyroid and parathyroid was not as pronounced in humans compared to the rabbit model. The readings from human tissue showed significantly lower overall impedance, greater overlap between thyroid and parathyroid EI and greater variability

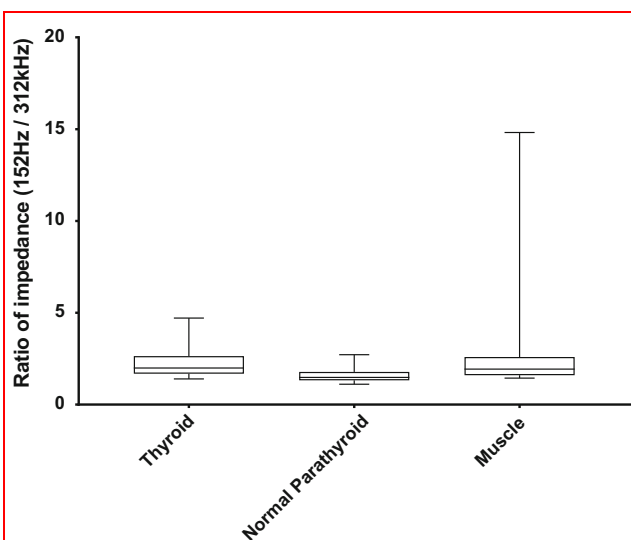


Fig. 4 Box and whisker plot comparing the ratio of in situ electrical impedance at two frequencies (152 Hz and 312 kHz) in thyroid, normal parathyroid, and muscle in humans. The ends of the box represent the 25th and 75th quartiles; the line in the box represents the median; the whiskers represent the minimum and maximum values

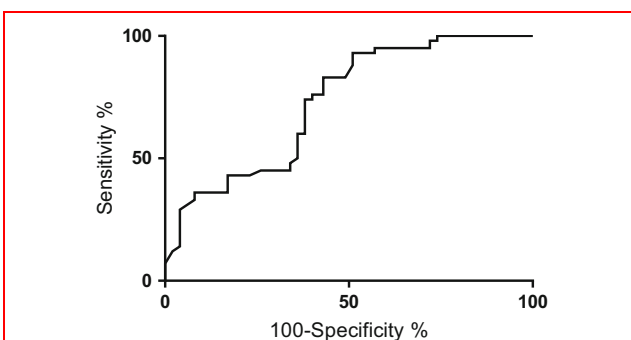


Fig. 5 ROC curve for normal parathyroid vs thyroid using the correlation with the normal parathyroid template

in amplitude of impedance compared to rabbit tissues. This variability was greater at low frequencies and improved as the frequency increased. For example, the impedance of normal thyroid at 76 Hz has a range of 530.30 Ω (176.83–707.13 Ω), whereas at 625 kHz the range is 94.61 Ω (72.89–167.50 Ω). The same is seen in the normal parathyroid where the range at 76 Hz is 433.68 Ω (138.99–572.67 Ω) and that at 625 kHz is 207.61 Ω (44.19–251.80 Ω).

However, there are similarities between the findings on humans and rabbits in relation to the shape of spectra. Normalising the data removed the variability in the amplitude but maintained the changes in impedance with frequency. In both the human and rabbit studies, the

parathyroid spectra have a much flatter curve than the thyroid, maintaining similar levels of impedance over the low frequencies which then dropped rapidly at higher frequencies. The thyroid spectra, in comparison, have a more inverse sigmoid shape with a rapid decline in the mid-range frequencies.

Template matching enables an understanding of the differences in the shapes of the curve and differentiation between parathyroid and thyroid tissues with a degree of confidence as proven by the ROC curve. It may be possible to increase the sensitivity and specificity of the test by weighting the areas of the spectra where the greatest differences in the curves are found. However, there does not appear to be enough difference between the spectra of normal and abnormal parathyroid glands to aid intraoperative diagnosis.

In concurrence with the findings in the rabbit study, *ex vivo* spectra had a higher impedance than the *in vivo* readings of the same tissues. This is most likely due to the change in temperature. Mean *in vivo* temperature was 36.3 $^{\circ}\text{C}$, and *ex vivo* temperature was 27.2 $^{\circ}\text{C}$. The overall shape of the spectra was maintained. At surgery, it is often difficult to determine gland viability and requirement for autotransplantation but a high impedance or an increase in impedance in the same gland after a period of time may indicate devascularisation. However, taking readings *ex vivo* may not give a true indication of what the EIS from an *in situ*, devascularised gland is as these glands may not drop their temperature as notably as there will still be transfer of heat from the body and operating lights.

Other limitations of this study include the reliance on surgical judgement on the nature of normal tissues *in situ* and the use of a template using internal study data. A standard parathyroid template should ideally be based on extensive analyses of histological specimens of normal and abnormal parathyroid glands, as has been done with cervical tissues [1]. In addition, the device and software were designed specifically for use in colposcopy and not for intraoperative use in the neck. Based on this study, some changes to facilitate intraoperative use such as having the display on a screen outside the operating field to decrease glare from the operating lights, reducing the size of the tip of the probe to improve contact with the tissues, in particular small parathyroid glands which may be smaller than the 5.5 mm diameter of the current tip, and developing a single-use disposable tip rather than a cover are being considered. In addition, to be used in clinical practice, real-time feedback from the device based on spectral analysis as to whether the tissue of interest is a parathyroid gland would have to be facilitated, just as the colposcopist receives feedback as to whether a tissue is abnormal and requires biopsy. These changes have the potential to improve the quality and reliability of the data collected.

This technology has the potential to provide a fast and simple answer for a surgeon to confirm the presence of parathyroid tissue. This could be used as an adjunct to the surgeon's expertise or alongside other identification techniques such as near-infrared fluorescence imaging. This would be of use in both thyroidectomy and neck explorations for hyperparathyroidism where parathyroid glands need to be identified for either preservation or resection. This also has potential to reduce risk of hypoparathyroidism in other head and neck surgeries such as laryngectomy or pharyngectomy. There may be a place for EIS to identify glands that should be considered for autotransplantation due to devascularisation, but this concept needs further investigation.

Acknowledgements Dr Peter Highfield, Technical Director of Zilico Ltd, provided technical support for this study.

Compliance with ethical standards

Conflict of interest SL Hillary declares no conflict of interest. BH Brown declares that he is the Academic Founder of Zilico Ltd. NJ Brown declares no conflict of interest. SP Balasubramanian declares no conflict of interest.

Ethical approval The study was approved by the appropriate institution and national research ethics committee.

Informed consent Informed, written consent was obtained from all individual participants included in the study.

Open Access This article is distributed under the terms of the Creative Commons Attribution 4.0 International License (<http://creativecommons.org/licenses/by/4.0/>), which permits unrestricted use, distribution, and reproduction in any medium, provided you give appropriate credit to the original author(s) and the source, provide a link to the Creative Commons license, and indicate if changes were made.

References

1. Tidy JA, Brown BH, Healey TJ, et al (2013) Accuracy of detection of high-grade cervical intraepithelial neoplasia using electrical impedance spectroscopy with colposcopy. *BJOG : an Int J Obstet Gynaecol* 120:400–410; discussion 410–401
2. Brown BH, Milnes P, Abdul S et al (2005) Detection of cervical intraepithelial neoplasia using impedance spectroscopy: a prospective study. *BJOG : an international journal of obstetrics and gynaecology* 112:802–806
3. Brown BH, Tidy JA, Boston K et al (2000) Relation between tissue structure and imposed electrical current flow in cervical neoplasia. *Lancet* 355:892–895
4. Abdul S, Brown BH, Milnes P et al (2006) The use of electrical impedance spectroscopy in the detection of cervical intraepithelial neoplasia. *Int J Gynecol Cancer* 16:1823–1832
5. Murdoch C, Brown BH, Hearnden V et al (2014) Use of electrical impedance spectroscopy to detect malignant and potentially malignant oral lesions. *Int J Nanomedicine* 9:4521–4532
6. Richter I, Alajbeg I, Boras VV et al (2015) Mapping Electrical Impedance Spectra of the Healthy Oral Mucosa: a Pilot Study. *Acta Stomatol Croat* 49:331–339
7. Pachek A, Mijailovic A, Yim S et al (2016) Tongue electrical impedance in amyotrophic lateral sclerosis modeled using the finite element method. *Clin Neurophysiol* 127:1886–1890
8. Aberg P, Nicander I, Hansson J et al (2004) Skin cancer identification using multifrequency electrical impedance—a potential screening tool. *IEEE Trans Biomed Eng* 51:2097–2102
9. Aberg P, Birgersson U, Elsner P et al (2011) Electrical impedance spectroscopy and the diagnostic accuracy for malignant melanoma. *Exp Dermatol* 20:648–652
10. Halter RJ, Schned A, Heaney J et al (2008) Electrical impedance spectroscopy of benign and malignant prostatic tissues. *J Urol* 179:1580–1586
11. Kerner TE, Paulsen KD, Hartov A et al (2002) Electrical impedance spectroscopy of the breast: clinical imaging results in 26 subjects. *IEEE Trans Med Imaging* 21:638–645
12. Keshtkar A, Salehnia Z, Keshtkar A et al (2012) Bladder cancer detection using electrical impedance technique (Tabriz Mark 1). *Patholog Res Int* 2012:470101
13. Mishra V, Bouayad H, Schned A et al (2012) Electrical impedance spectroscopy for prostate cancer diagnosis. *Conf Proc IEEE Eng Med Biol Soc* 2012:3258–3261
14. Stojadinovic A, Nissan A, Shriver CD et al (2008) Electrical impedance scanning as a new breast cancer risk stratification tool for young women. *J Surg Oncol* 97:112–120
15. Edafe O, Balasubramanian SP (2017) Incidence, prevalence and risk factors for post-surgical hypocalcaemia and hypoparathyroidism. *Gland Surg* 6:S59–S68
16. Vadiveloo T, Donnan PT, Leese CJ et al (2019) Increased mortality and morbidity in patients with chronic hypoparathyroidism: A population-based study. *Clin Endocrinol (Oxf)* 90:285–292
17. Antakia R, Brown BH, Highfield PE et al (2016) Electrical Impedance Spectroscopy to Aid Parathyroid Identification and Preservation in Central Compartment Neck Surgery: A Proof of Concept in a Rabbit Model. *Surg Innov* 23:176–182
18. Edd JF, Horowitz L, Rubinsky B (2005) Temperature dependence of tissue impedivity in electrical impedance tomography of cryosurgery. *IEEE transactions on bio-medical engineering* 52:695–701
19. Clinicaltrials.gov EIS in Thyroid and Parathyroid Surgery, 2016.

Publisher's Note Springer Nature remains neutral with regard to jurisdictional claims in published maps and institutional affiliations.